ARMY RESEARCH LABORATORY

Efficient Maximum Likelihood Estimation for Multiple and Coupled Harmonics

Douglas Lake

ARL-TR-2014

December 1999

The findings in this report are not to be construed as an official Department of the Army position unless so designated by other authorized documents.

Citation of manufacturer's or trade names does not constitute an official endorsement or approval of the use thereof.

Destroy this report when it is no longer needed. Do not return it to the originator.

Army Research Laboratory

Adelphi, MD 20783-1197

ARL-TR-2014 **December 1999**

Efficient Maximum Likelihood Estimation for Multiple and Coupled Harmonics

Douglas Lake

Sensors and Electron Devices Directorate

Abstract

The maximum likelihood estimates (MLEs) and Cramer-Rao bounds (CRBs) for parameters of harmonics in Gaussian noise have been well studied. If the phase of the signal is defined in the middle of the time interval rather than at the beginning (as is more common), the information matrix is approximately diagonal, and the formulation and analysis of the MLEs and CRBs are simplified. More significantly, this simple modification decouples the estimation of phase and frequency and leads to efficient MLE gradient descent algorithms. In this report, these MLE procedures and CRB analysis are presented for the multiple and coupled harmonic case, as well as for colored noise. A new criterion on the required sample size is presented to give uniform bounds on the accuracy of diagonal information matrix approximation; uniform bounds are needed to ensure the effectiveness of the gradient descent methods. These methods are demonstrated on real data from battlefield acoustic sensors, where they can be used to help identify targets of interest, such as tanks or trucks.

Contents

Figures

1. Introduction

The Cramer-Rao bounds (CRBs) for estimating the parameters of harmonics in Gaussian white noise were first presented by Rife and Boorstyn [1,2]. More recently, the results have been presented by Stoica et al [3] and Porat [4] and extended to include multiplicative noise by Zhou and Giannakis [5]. The estimation algorithms presented by Stoica et al [3] do not exploit a key observation made originally by Rife and Boorstyn [1], and more recently by Porat [4], on the effect of defining the phase of the signal in the middle of the time interval rather than at the beginning, which is more commonly done. Perhaps some reluctance in using the less common definition is due to the misperception (as in Porat [4]) that odd and even numbers of samples need to be treated separately. With the phase in the middle of the time interval, the information matrix is approximately diagonal as compared to the results in Stoica et al [3] and elsewhere, where the phase and frequency estimates have significant correlation, and the formulation and analysis of the maximum likelihood estimates (MLEs) and the CRBs are simplified. More significantly, this simple modification decouples the estimations of phase and frequency and leads to more efficient MLE gradient descent algorithms. To ensure the effectiveness of the gradient descent algorithms, I suggest a new criterion for the required sample size that gives uniform bounds on the accuracy of diagonal information matrix approximation. In this report, these MLE methods and CRB analysis are presented for the multiple and coupled harmonic cases, as well as for colored noise, with application to real data from battlefield acoustic sensors. These approaches and analysis provide valuable insights into the problem of target identification and the design of computationally efficient battlefield acoustic systems.

2. Harmonic Signal Models

The classic real single harmonic signal model for the signal $s(t)$ at continuous time t is

$$s(t) = A\cos(\omega t + \phi) \,, \tag{1}$$

where $A > 0$ is the amplitude, ω is the angular frequency, and ϕ is the phase. The frequency $f = \omega/(2\pi)$ is often the natural parameter, but using ω helps simplify the notation, and results can be readily applied to both. It is sometimes preferable to write equation (1) as

$$s(t) = u\cos(\omega t) + v\sin(\omega t) \,, \tag{2}$$

where $u = A\cos(\phi)$ and $v = -A\sin(\phi)$ are the in-phase and quadrature-phase components of the signal. The parameters in equation (2) can be transformed to those in equation (1) via

$$\begin{aligned} A &= (u^2 + v^2)^{1/2} \,, \\ \phi &= \arctan(-v, u) \,, \end{aligned} \tag{3}$$

where arctan is the four-quadrant arc tangent function (MATLAB function ATAN2). The parameters of this model will be denoted by $\boldsymbol{\theta} = (A, \phi, \omega)$ or $\boldsymbol{\theta} = (u, v, f)$.

The multiple harmonic model generalizes equation (1) as

$$s(t) = \sum_{k=1}^{m} A_k \cos(\omega_k t + \phi_k) \tag{4}$$

and equation (2) as

$$s(t) = \sum_{k=1}^{m} u_k \cos(\omega_k t) + v_k \sin(\omega_k t) \,, \tag{5}$$

so that the multiple harmonic parameters are $\boldsymbol{\theta} = (\mathbf{A}, \boldsymbol{\phi}, \boldsymbol{\omega})$ in equation (4) and $\boldsymbol{\theta} = (\mathbf{u}, \mathbf{v}, \boldsymbol{\omega})$ in equation (5). An important model that is a special case of equation (4) is the coupled harmonic signal model

$$s(t) = \sum_{k=1}^{m} A_k \cos(h_k \omega t + \phi_k) \,, \tag{6}$$

where ω is called the *fundamental frequency*, h_k is an integer indicating the kth harmonic number (assumed known), and A_k and ϕ_k are the amplitude and phase of the kth harmonic. It is clear that equation (6) is equivalent to equation (4) with $\omega_k = h_k\omega$, but the number of parameters has been reduced ($2m + 1$ instead of $3m$) and will be denoted by $\boldsymbol{\theta} = (\mathbf{A}, \boldsymbol{\phi}, \omega)$ or $\boldsymbol{\theta} = (\mathbf{u}, \mathbf{v}, \omega)$.

The data sequence $X[m]$ received at the acoustic sensor (for the application presented in sect. 7) is an equally spaced sampled version of the continuous-time model:

$$X[m] = s(t(m)) + Z[m] \,, \tag{7}$$

where $t(m)$ is the time of the mth sample and $Z[m]$ is the cumulative additive noise. Without loss of generality, it is assumed that the sampling rate is $T = 1$ so that difference $t(m) - t(m-1) = 1$ for all m, and the frequencies are normalized so that Nyquist is π. In order to ensure that the parameters are identifiable, it is required that $A > 0$ and $0 < \omega < \pi$ ($0 < f < 1/2$).

Let $\mathbf{y} = (y_1, y_2, \ldots, y_n)^T$ be a vector denoting a given set of n samples from the data over a particular time window. The time reference in equation (1) can always be redefined, so without loss of generality, we can assume that $y_i = X[t(i)]$. The model in equation (7) can be written as

$$\mathbf{x} = \mathbf{s}(\theta) + \mathbf{z} \,, \tag{8}$$

where

$$s_i(\theta) = A\cos(\omega t(i) + \phi) \,. \tag{9}$$

First consider the case where Z is assumed white, so that the noise vector $\mathbf{z}$ is multivariate Gaussian $N_n(0, \sigma^2\mathbf{I})$; that is, $z_1, z_2, \ldots, z_n$ are independently and identically distributed (i.i.d.) Gaussian with variance σ^2. To simplify the analysis, I assume the variance is known, although all the results presented are equally valid in the unknown case. In this case, the MLE maximizes

$$\log(L(\mathbf{y}, \theta)) = -\frac{1}{2\sigma^2}\|\mathbf{y} - \mathbf{s}(\theta)\|^2 - n/2\log(2\pi\sigma^2) \,, \tag{10}$$

which is equivalent to minimizing the residual sum of squares

$$SS(\theta) = \|\mathbf{y} - \mathbf{s}(\theta)|^2 = \|\mathbf{e}\|^2 \,, \tag{11}$$

where $\mathbf{e} = \mathbf{e}(\theta)$ is the residual error.

The information matrix for estimating the parameters of $\mathbf{s}(\theta)$ is given by

$$\mathbf{I}(\theta) = \frac{1}{\sigma^2}\frac{\partial \mathbf{s}}{\partial \theta}^T \frac{\partial \mathbf{s}}{\partial \theta} \,, \tag{12}$$

where

$$\left[\frac{\partial \mathbf{s}}{\partial \theta}\right]_{ij} = \frac{\partial \mathbf{s}_i}{\partial \theta_j} \tag{13}$$

is a matrix of first derivatives.

Calculations of the CRBs for the harmonic signal models are somewhat complicated but involve the straightforward use of trigonometric identities and summation formulas. While exact information matrices can be readily calculated, interpretation is only practical if approximations are used for large sample sizes n. Approximate results are obtained via the standard summation formula (and its first and second derivatives), which for arbitrary time indices is

$$\frac{1}{n}\sum_{i=1}^{n}\cos(\omega t(i)+\phi) = \cos(\phi + (t(1)+(n-1)/2)\omega)\epsilon(\omega/2)\,, \tag{14}$$

where

$$\epsilon(\omega) = \frac{\sin(n\omega)}{n\sin(\omega)} \tag{15}$$

is the normalized *Dirichlet kernel*. A classic result, first presented by Rife and Boorstyn [1] (for the single-tone complex case) and also discussed in detail by Kay [6], is the CRB for the single harmonic model, where the information matrix is approximately

$$\mathbf{I}(A,\phi,\omega) \approx \rho \begin{bmatrix} \frac{n}{A^2} & 0 & 0 \\ 0 & n & \sum_{i=1}^{n} t(i) \\ 0 & \sum_{i=1}^{n} t(i) & \sum_{i=1}^{n} t(i)^2 \end{bmatrix}, \tag{16}$$

where $\rho = A^2/(2\sigma^2)$ is the signal-to-noise ratio (SNR). For Fourier analysis and other applications, the time samples are taken to be $t(i) = i-1$ or $t(i) = i$, so that the phase is associated with the beginning of the time window. For $t(i) = i-1$, inverting equation (12) leads to the approximate CRBs

$$\begin{aligned} \mathrm{CRB}[\hat{A}] &\approx \frac{A^2}{n\rho} = \frac{2\sigma^2}{n}\,, \\ \mathrm{CRB}[\hat{\phi}] &\approx \frac{2(2n-1)}{(n(n+1)\rho}\,, \end{aligned} \tag{17}$$

for phase and amplitude and

$$\mathrm{CRB}[\hat{\omega}] \approx \frac{12}{n(n^2-1)\rho} \approx \frac{12}{n^3\rho} \tag{18}$$

for frequency. It also leads to

$$\mathrm{CRB}[\hat{f}] = \frac{1}{(2\pi)^2}\mathrm{CRB}[\hat{\omega}] \approx \frac{12}{(2\pi)^2 n(n^2-1)\rho} \tag{19}$$

for the alternative definition of frequency.

As equation (12) shows, the approximate information matrix can be made diagonal if the sum of the time samples is 0. This can be accomplished with $t(i) = i - (n+1)/2$ and corresponds to associating the phase with the middle of the time window. In this case,

$$\mathbf{I}(A,\phi,\omega) \approx n\rho \begin{bmatrix} \frac{1}{A^2} & 0 & 0 \\ 0 & 1 & 0 \\ 0 & 0 & \frac{1}{12}(n^2-1) \end{bmatrix}, \tag{20}$$

which can be readily inverted to give approximate CRBs that agree with equation (17), except, notably, for

$$\mathrm{CRB}[\hat{\phi}] \approx \frac{1}{n\rho}, \tag{21}$$

which, as first noted by Rife and Boorstyn [1] is the minimum value for any location of phase and is equal to the CRB when frequency is known.

The bound for estimating the phase in the middle of the time window is a factor of $2(2n-1)/(n+1)$, or roughly four times smaller than the bound for estimating the phase at the beginning of the time window. To see why, note that the estimate of phase at the first sample and the phase at the middle of the samples, denoted by $\hat{\phi}_0$ and $\hat{\phi}_{1/2}$, respectively, are related by

$$\hat{\phi}_0 = \hat{\phi}_{1/2} - (n-1)\hat{\omega}/2, \tag{22}$$

so that for minimal variance unbiased estimators,

$$\mathrm{Var}[\hat{\phi}_0] = \mathrm{Var}[\hat{\phi}_{1/2}] + \mathrm{Var}[(n-1)\omega/2] = \frac{1}{n\rho} + \frac{(n-1)^2}{4}\frac{12}{n(n^2-1)\rho} = \frac{2(2n-1)}{n(n+1)\rho}, \tag{23}$$

which agrees with equation (17).

The reduction in variance of the estimate of $\phi_{1/2}$ should not be misconstrued as somehow a better overall estimate of the signal. The equality in equation (22) (or similar relationships) can be used in reverse, to go from equation (21) to equation (17) (or other CRBs), so if one is interested in ϕ_0 or any other location of phase, the variance will increase and nothing will change that. In terms of ease of analysis for the single harmonic case, the

tradeoff in using the phase in the middle of the window is between inverting a 2×2 matrix in equation (16) and evaluating $\sum t(i)^2$ for nonstandard time indices (i.e., $t(i) = i-(n+1)/2$ instead of $t(i) = i-1$). The preference, debatable at best, is certainly not a big issue. However, with more complicated analysis such as that presented by Stoica et al [3] and Zhou and Giannakis [5], the small increment of simplicity in this approach is probably welcome. Unless noted otherwise, the results presented here reflect the phase defined in the middle of the time window. Besides easing the analysis, it is shown in section 5 that the diagonality of the information matrices leads to more efficient estimation procedures, including instances in which the decoupling of the frequency and phase estimates is crucial.

An approximate CRB for harmonic signal models can be made more explicit through use of an asymptotic Cramer-Rao bound (ACRB), which can be obtained from an asymptotic information matrix of normalized parameters. For example, in the case of a single harmonic, the ACRBs are given by

$$\begin{aligned} \text{ACRB}[\hat{A}] &= 2\sigma^2 , \\ \text{ACRB}[\hat{\phi}] &= \frac{1}{\rho} , \\ \text{ACRB}[\hat{\omega}] &= \frac{12}{\rho} , \end{aligned} \tag{24}$$

and are obtained by inverting

$$\mathbf{I}_\infty(A,\phi,\omega) = \lim_{n\to\infty} \mathbf{I}_n(n^{-1/2}A, n^{-1/2}\phi, n^{-3/2}\omega) = \rho \begin{bmatrix} \frac{1}{A^2} & 0 & 0 \\ 0 & 1 & 0 \\ 0 & 0 & \frac{1}{12} \end{bmatrix} , \tag{25}$$

where $\mathbf{I}_\infty$ is the asymptotic information matrix. In this report, each CRB given as an approximation is with the understanding of this relationship to the ACRB.

Stoica et al [3] have shown that all the cross-terms in the asymptotic information matrix for the multiple harmonic signal model involving different harmonics are zero, so the generalization of equation (20) is still approximately diagonal,

$$I(\mathbf{A},\boldsymbol{\phi},\boldsymbol{\omega}) \approx \frac{n}{2\sigma^2} \begin{bmatrix} \mathbf{I} & \mathbf{0} & \mathbf{0} \\ \mathbf{0} & \mathbf{D} & \mathbf{0} \\ \mathbf{0} & \mathbf{0} & \frac{1}{12}n^2\mathbf{D} \end{bmatrix} , \tag{26}$$

where

$$\mathbf{D} = \text{diag}(A_1^2, \ldots, A_m^2) \tag{27}$$

is a diagonal matrix. So the CRBs for the multiple case are approximately all the same as the single case; that is,

$$\begin{aligned} \text{CRB}[\hat{A}_k] &\approx \frac{2}{n}\sigma^2 , \\ \text{CRB}[\hat{\phi}_k] &\approx \frac{1}{n\rho_k} , \\ \text{CRB}[\hat{\omega}_k] &\approx \frac{12}{n^3\rho_k} , \end{aligned} \tag{28}$$

where $\rho_k = A_k^2/(2\sigma^2)$ is the SNR of the kth harmonic.

For the coupled harmonic case, the cross-terms are all asymptotically zero, and the information matrix becomes

$$I(\mathbf{A}, \boldsymbol{\phi}, \omega) \approx \frac{n}{2\sigma^2} \begin{bmatrix} \mathbf{I} & \mathbf{0} & \mathbf{0} \\ \mathbf{0} & \mathbf{D} & \mathbf{0} \\ \mathbf{0} & \mathbf{0} & \frac{1}{12}n^2 \sum_{k=1}^{m} h_k^2 A_k^2 \end{bmatrix} , \tag{29}$$

so that the CRBs for amplitude and phase are the same as in equation (28). The CRB for fundamental frequency is

$$\text{CRB}[\hat{\omega}] \approx \frac{12}{n^3} \left(\sum_{k=1}^{m} h_k^2 \rho_k \right)^{-1} , \tag{30}$$

which agrees with the result in Swami and Ghogho [7], which was obtained by considering the coupled harmonic model as a constrained version of the multiple case.

3. Summation Formulas for Well-Resolved Frequencies

All the entries of the information matrices for harmonic signal models involve summations of the form

$$\delta_p(\omega_1, \omega_2, \phi_1, \phi_2) = \sum_{i=1}^{n} t(i)^p \cos(\omega_1 t(i) + \phi_1) \cos(\omega_2 t(i) + \phi_2) \tag{31}$$

and

$$\epsilon_p(\omega, \phi) = \frac{1}{n^{p+1}} \sum_{i=1}^{n} t(i)^p \cos(\omega t(i) + \phi) \tag{32}$$

for $p = 0, 1, 2$, which are related by

$$\delta_p(\omega_1, \omega_2, \phi_1, \phi_2) = \frac{1}{2} n^{p+1} \left(\epsilon_p(\omega_1 - \omega_2, \phi_1 - \phi_2) + \epsilon_p(\omega_1 + \omega_2, \phi_1 + \phi_2)\right) \tag{33}$$

with the use of a standard trigonometric identity. Using the above notation, one finds that

$$\begin{aligned}
\frac{\partial \mathbf{s}^T}{\partial A_i} \frac{\partial \mathbf{s}}{\partial A_j} &= \delta_0(\omega_i, \omega_j, \phi_i, \phi_j) \,, \\
\frac{\partial \mathbf{s}^T}{\partial \phi_i} \frac{\partial \mathbf{s}}{\partial \phi_j} &= A_i A_j \delta_0(\omega_i, \omega_j, \phi_i + \pi/2, \phi_j + \pi/2) \,, \\
\frac{\partial \mathbf{s}^T}{\partial \omega_i} \frac{\partial \mathbf{s}}{\partial \omega_j} &= A_i A_j \delta_2(\omega_i, \omega_j, \phi_i + \pi/2, \phi_j + \pi/2) \,, \\
\frac{\partial \mathbf{s}^T}{\partial A_i} \frac{\partial \mathbf{s}}{\partial \phi_j} &= A_j \delta_0(\omega_i, \omega_j, \phi_i, \phi_j + \pi/2) \,, \\
\frac{\partial \mathbf{s}^T}{\partial A_i} \frac{\partial \mathbf{s}}{\partial \omega_j} &= A_j \delta_1(\omega_i, \omega_j, \phi_i, \phi_j + \pi/2) \,, \\
\frac{\partial \mathbf{s}^T}{\partial \phi_i} \frac{\partial \mathbf{s}}{\partial \omega_j} &= A_i A_j \delta_1(\omega_i, \omega_j, \phi_i + \pi/2, \phi_j + \pi/2) \,,
\end{aligned} \tag{34}$$

are the exact terms of the information matrix for multiple harmonics. Similarly,

$$\begin{aligned}
\frac{\partial \mathbf{s}^T}{\partial A_i}\frac{\partial \mathbf{s}}{\partial A_j} &= \delta_0(h_i\omega, h_j\omega, \phi_i, \phi_j) \ , \\
\frac{\partial \mathbf{s}^T}{\partial \phi_i}\frac{\partial \mathbf{s}}{\partial \phi_j} &= A_i A_j \delta_0(h_i\omega, h_j\omega, \phi_i + \pi/2, \phi_j + \pi/2) \ , \\
\frac{\partial \mathbf{s}^T}{\partial \omega}\frac{\partial \mathbf{s}}{\partial \omega} &= \sum_{i=1}^{m}\sum_{j=1}^{m} h_i h_j A_i A_j \delta_2(h_i\omega, h_j\omega, \phi_i + \pi/2, \phi_j + \pi/2) \ , \\
\frac{\partial \mathbf{s}^T}{\partial A_i}\frac{\partial \mathbf{s}}{\partial \phi_j} &= A_j \delta_0(h_i\omega, h_j\omega, \phi_i, \phi_j + \pi/2) \ , \\
\frac{\partial \mathbf{s}^T}{\partial A_i}\frac{\partial \mathbf{s}}{\partial \omega} &= \sum_{j=1}^{m} h_j A_j \delta_1(h_i\omega, h_j\omega, \phi_i, \phi_j + \pi/2) \ , \\
\frac{\partial \mathbf{s}^T}{\partial \phi_i}\frac{\partial \mathbf{s}}{\partial \omega} &= h_i A_i \sum_{j=1}^{m} h_j A_j \delta_1(h_i\omega, h_j\omega, \phi_i + \pi/2, \phi_j + \pi/2) \ ,
\end{aligned} \tag{35}$$

are the exact terms of the information matrix for coupled harmonics. Approximations of the information matrices of harmonic signal models ($\omega_i = h_i\omega$ for coupled harmonics) require that

$$\begin{aligned}
\delta_p(\omega_i, \omega_j, \phi_i, \phi_j) &\approx 0, \\
\delta_p(\omega_i, \omega_i, \phi_i, \phi_i) &\approx \frac{1}{2} n^{p+1} \epsilon_p(0, 0) \ ,
\end{aligned} \tag{36}$$

for $1 \leq i < j \leq m$. The approximations in equation (36) are valid if the summations in equation (32) are near 0 for all combinations of their sums and differences, $\omega_i \pm \omega_j$, except for $\omega_i = \omega_j$. If this requirement is met (under some specified criteria), the frequencies will be called *well resolved*. For a given set of frequencies, a natural question is how large n needs to be in order for them to be well resolved.

Using two-term expansion of the exact information matrix about the approximation in equation (26), Porat [4] shows that for multiple harmonics, the first-order accuracy of the approximate CRBs in equation (28) is dependent on the value of the normalized Dirichlet kernel in equation (14). The normalized Dirichlet kernel attains a maximum of 1 at $\omega = 0$ (and multiples of π) and has main lobes between $\pm\pi/n$ and $\pi \pm \pi/n$. A reasonable requirement for n is that these critical values of ω lie outside these main lobes; this leads to Porat's requirement [4],

$$n \geq \max_{1 \leq i < j \leq m} \left(\frac{\pi}{\omega_i}, \frac{\pi}{\pi - \omega_i}, \frac{2\pi}{|\omega_i - \omega_j|}, \frac{2\pi}{2\pi - \omega_i - \omega_j} \right) , \tag{37}$$

which is a simple rule of thumb for estimating a sufficient sample size. While equation (37) controls the bounds on the variances of the parameters via equation (49), it is also important that covariance terms be small, such as when using the method of scoring. The correlations between frequency and both phase and amplitude are on the order of ϵ_1 and $\epsilon_1(\pi/n) \approx -1/\pi = -0.3183$ for the minimal sample size to satisfy equation (37). This may not be small enough for some applications, and equation (37) would underestimate the required sample size in this instance. I propose a supplemental criterion for calling frequencies well resolved that ensures that the summations in equation (32) are uniformly small.

Equation (14) shows that, more specifically, the denominator of equation (15) must be large in order for ϵ_0 to be small. This motivates calling $n\sin(\omega)$ the *frequency resolution* and defining its inverse,

$$\Delta(\omega) = \frac{1}{n\sin(\omega)}, \tag{38}$$

which could be called the *frequency coarseness*. With the phase defined in the middle of the time window, $t(1) = -(n-1)/2$, and equation (14) simplifies to

$$\epsilon_0(\omega, \phi) = \cos(\phi)\epsilon(\omega/2) = \cos(\phi)\sin(n\omega/2)\Delta(\omega/2)\ , \tag{39}$$

which is valid for n, both odd and even. A particular case of equation (39) is

$$\epsilon_0(\omega, -\pi/2) = \sum_{i=1}^{n} \sin(\omega t(i)) = 0 \tag{40}$$

for all ω, which is also evident by the antisymmetry of the time samples and the symmetry of the sine function around 0. Differentiating $\epsilon_0(\omega, \phi - \pi/2)$ leads to

$$\epsilon_1(\omega, \phi) = \frac{1}{2}\sin(\phi)\Delta(\omega/2)\left(-\cos(n\omega/2) + \sin(n\omega/2)\cos(\omega/2)\Delta(\omega/2)\right)\ , \tag{41}$$

which, by the use of l'Hopital's rule, can be shown to be continuous at $\omega = 0$, where $\epsilon_1(0, \phi) = 0$. Similarly, differentiating $\epsilon_1(\omega, \phi - \pi/2)$ leads to

$$\begin{aligned}\epsilon_2(\omega, \phi) \ = \ & \frac{1}{4}\cos(\phi)\Delta(\omega/2)\left(-\sin(n\omega/2) + 2\cos(n\omega/2)\cos(\omega/2)\Delta(\omega/2)\right. \\ & \left. - \sin(n\omega/2)(1 + \cos^2(n\omega/2))\Delta^2(\omega/2)\right)\ ,\end{aligned} \tag{42}$$

which is also continuous at $\omega = 0$, where, for example, $\epsilon_2(0,0) = (1 - n^{-2})/12$.

It is easy to find the following bounds,

$$\begin{aligned} |\epsilon_0(\omega,\phi)| &\leq \Delta(\omega/2)\,, \\ |\epsilon_1(\omega,\phi)| &\leq (\Delta(\omega/2)+\Delta^2(\omega/2))/2\,, \\ |\epsilon_2(\omega,\phi)| &\leq (\Delta(\omega/2)+2\Delta^2(\omega/2)+2\Delta^3(\omega/2))/4\,, \end{aligned} \tag{43}$$

which, for all pertinent $\omega > 0$ and n already satisfying equation (37), leads to the simple uniform bound on equation (32),

$$|\epsilon_p(\omega,\phi)| \leq \Delta(\omega/2), \tag{44}$$

and, ultimately,

$$|\delta_p(\omega_1,\omega_2,\phi_1,\phi_2)| \leq n^{p+1}\Delta(\omega/2)\,, \tag{45}$$

for $\omega_1 \neq \omega_2$ in equation (33). So perhaps better criteria for selecting n are to require that Δ be small and to ensure the uniform bounds in equations (44) and (45), which lead to

$$\Delta(\boldsymbol{\omega}) = \min_{1\leq i<j\leq m} [\Delta(\omega_i), \Delta(|\omega_i-\omega_j|/2), \Delta((\omega_i+\omega_j)/2)] < \epsilon \tag{46}$$

for some specified tolerance $\epsilon > 0$. These criteria are equivalent to

$$n \geq \max_{1\leq i<j\leq m} \frac{1}{\epsilon}\left[\frac{1}{\sin(\omega_i)}, \frac{1}{\sin(|\omega_i-\omega_j|/2)}, \frac{1}{\sin((\omega_i+\omega_j)/2)}\right]\,, \tag{47}$$

which is nearly the same as

$$n \geq \max_{1\leq i<j\leq m} \frac{1}{\epsilon}\left(\frac{1}{\omega_i}, \frac{1}{\pi-\omega_i}, \frac{2}{|\omega_i-\omega_j|}, \frac{2}{2\pi-\omega_i-\omega_j}\right)\,, \tag{48}$$

when one uses approximations of the sine function near 0 and π. Note that equation (48) is a generalization of equation (37), with $\epsilon = 1/\pi$. So in order to get stricter requirements on the sample size, the tolerance should be selected so that $\epsilon < 1/\pi$.

In terms of Δ, the expressions given by Porat [4] for multiple harmonics become

$$\begin{aligned} \mathrm{CRB}[\hat{A}_k] &= \frac{2\sigma^2}{n}\Big\{1-\cos(2\phi_k)\sin(n\omega_k)\Delta(\omega_k)+o[\Delta(\boldsymbol{\omega})]\Big\}\,, \\ \mathrm{CRB}[\hat{\phi}_k] &= \frac{1}{n\rho_k}\Big\{1+\cos(2\phi_k)\sin(n\omega_k)\Delta(\omega_k)+o[\Delta(\boldsymbol{\omega})]\Big\}\,, \end{aligned} \tag{49}$$

for amplitudes and phases, and

$$\mathrm{CRB}[\hat{\omega}_k] = \frac{12}{n^3\rho_k}\Big\{1+3\cos(2\phi_k)\sin(n\omega_k)\Delta(\omega_k)+o[\Delta(\boldsymbol{\omega})]\Big\} \tag{50}$$

for frequency, where $o[\Delta(\boldsymbol{\omega})]$ is a term that goes to 0 faster than $\Delta(\boldsymbol{\omega})$. The analogous expression for the CRB between frequency and phase of the same harmonic, for example, is

$$\mathrm{CRB}[\hat{\phi}_k, \hat{\omega}_k] = \frac{2}{n^2 \rho_k} \cos(n\omega_k)\Delta(\omega_k) + o(\Delta(\boldsymbol{\omega})) \;, \tag{51}$$

which suggests the appropriateness of equation (46) if this term needs to be near 0.

The requirements for well-resolved frequencies generally apply to the coupled harmonic signal model, and expressions like equation (49) are readily available for amplitudes and phases. The analogous expression of equation (50) for fundamental frequency is not especially illuminating, but the ratio of the second term to the first term is seen to be on the order of $\Delta(\boldsymbol{\omega})$ when one notes that

$$\begin{aligned} \left| \frac{\partial \mathbf{s}^T}{\partial \omega} \frac{\partial \mathbf{s}}{\partial \omega} - \frac{1}{2} n^3 \epsilon(0,0) \sum_{i=1}^{m} h_i^2 A_i^2 \right| &\leq n^3 \Delta(\boldsymbol{\omega}) \sum_{i=1}^{m} \sum_{j=1}^{m} h_i h_j A_i A_j \\ &= n^3 \Delta(\boldsymbol{\omega}) \left(\sum_{i=1}^{m} h_i A_i \right)^2 \\ &\leq m n^3 \Delta(\boldsymbol{\omega}) \sum_{i=1}^{m} h_i^2 A_i^2 \;, \end{aligned} \tag{52}$$

where the last step follows from the Cauchy-Schwarz inequality. So the first-order approximations for the coupled harmonic case are still on the order of $\Delta(\boldsymbol{\omega})$, and the choice of n by equation (46) or (47) is still appropriate.

4. Maximum Likelihood Estimation for Multiple and Coupled Harmonics

Since equations (6) and (1) are special cases of equation (4), we present the MLE procedures in terms of the multiple harmonic case. The gradient descent methods for equation (6) are sufficiently distinct and will be treated separately. With equation (5), the multiple harmonical parameter estimation problem can be written as a linear model

$$\mathbf{y} = \mathbf{X}\beta + \mathbf{z}\,, \tag{53}$$

where $\mathbf{X} = \mathbf{X}(\omega)$ is an $n \times 2m$ matrix and the parameter

$$\beta = \begin{bmatrix} \mathbf{u} \\ \mathbf{v} \end{bmatrix} \tag{54}$$

is a $2m \times 1$ vector. One can write $\mathbf{X} = [\mathbf{C}\ \mathbf{S}]$, where $\mathbf{C}$ and $\mathbf{S}$ are $n \times m$ matrices given by

$$\begin{aligned} \mathbf{C}_{ij} &= \cos[\omega_j t(i)] \\ \mathbf{S}_{ij} &= \sin[\omega_j t(i)]\,, \end{aligned} \tag{55}$$

so that equation (53) becomes

$$\mathbf{y} = \mathbf{C}\mathbf{u} + \mathbf{S}\mathbf{v} + \mathbf{z} \tag{56}$$

in terms of $\mathbf{u}$ and $\mathbf{v}$. For Gaussian white noise, the MLE of β for fixed frequencies ω is also the least-squares estimator (LSE), given by

$$\hat{\beta} = \hat{\beta}(\omega) = (\mathbf{X}^T\mathbf{X})^{-1}\mathbf{X}^T\mathbf{y} \tag{57}$$

when the standard method of least squares is used. The MLEs of $\mathbf{u}$ and $\mathbf{v}$ are readily found with equation (54), and

$$\begin{aligned} \hat{A}_k &= (\hat{u}_k^2 + \hat{v}_k^2)^{1/2}\,, \\ \hat{\phi}_k &= \arctan(-\hat{v}_k, \hat{u}_k) \end{aligned} \tag{58}$$

are the MLEs of the amplitude and phase. Finding the MLE of θ requires some sort of search, either grid or gradient descent, to find the minimum

value of equation (11). So, for moderate m, finding the MLE of the harmonical parameters is potentially computationally expensive because of the matrix inversion in equation (89). Fortunately, with the phase defined in the middle of the time window, $\mathbf{X}^T\mathbf{X}$ is block diagonal and it decouples the estimation of $\mathbf{u}$ and $\mathbf{v}$. Moreover, $\mathbf{X}^T\mathbf{X}$ is approximately diagonal, and accurate estimates can be obtained without inversion.

In terms of $\mathbf{C}$ and $\mathbf{S}$,

$$\mathbf{X}^T\mathbf{X} = \begin{bmatrix} \mathbf{C}^T\mathbf{C} & \mathbf{S}^T\mathbf{C} \\ \mathbf{C}^T\mathbf{S} & \mathbf{S}^T\mathbf{S} \end{bmatrix} = \begin{bmatrix} \mathbf{C}^T\mathbf{C} & \mathbf{0} \\ \mathbf{0} & \mathbf{S}^T\mathbf{S} \end{bmatrix} . \tag{59}$$

The estimation of $\mathbf{u}$ and $\mathbf{v}$ decouple into

$$\begin{aligned} \hat{\mathbf{u}} &= (\mathbf{C}^T\mathbf{C})^{-1}\mathbf{C}^T\mathbf{y} , \\ \hat{\mathbf{v}} &= (\mathbf{S}^T\mathbf{S})^{-1}\mathbf{S}^T\mathbf{y} , \end{aligned} \tag{60}$$

which is computationally more efficient than using equation (57) if the phase is not defined in the middle of the time window (inverting two $m \times m$ matrices is better than inverting one $2m \times 2m$ matrix). For single harmonics, the exact MLE can be easily found, because

$$\begin{aligned} \mathbf{C}^T\mathbf{C} &= \frac{n}{2}(1 + \epsilon(\omega)) , \\ \mathbf{S}^T\mathbf{S} &= \frac{n}{2}(1 - \epsilon(\omega)) , \end{aligned} \tag{61}$$

where $\epsilon(\omega)$ is given by equation (15). So

$$\begin{aligned} \hat{\mathbf{u}} &= \frac{1}{1 + \epsilon(\omega)}\frac{2}{n}\mathbf{C}^T\mathbf{y} , \\ \hat{\mathbf{v}} &= \frac{1}{1 - \epsilon(\omega)}\frac{2}{n}\mathbf{S}^T\mathbf{y} \end{aligned} \tag{62}$$

is the exact MLE from equation (60).

For multiple harmonics, the exact entries of the matrices to be inverted are

$$\begin{aligned} \left[\mathbf{C}^T\mathbf{C}\right]_{ij} &= \delta_0(\omega_i, \omega_j, 0, 0) , \\ \left[\mathbf{S}^T\mathbf{S}\right]_{ij} &= \delta_0(\omega_i, \omega_j, -\pi/2, -\pi/2) , \end{aligned} \tag{63}$$

which for well-resolved frequencies leads to the well-known result

$$\mathbf{X}^T\mathbf{X} \approx \frac{n}{2}\mathbf{I}, \tag{64}$$

with the use of the approximations in equation (36). So accurate approximate MLE solutions without matrix inversion for $\mathbf{u}$ and $\mathbf{v}$ are

$$\hat{\boldsymbol{\beta}} \approx \frac{2}{n}\mathbf{X}^T\mathbf{y} \,, \tag{65}$$

which in the single harmonic case is equivalent to setting $\epsilon(\omega)$ to 0 in equation (62). An alternative approximate MLE for the multiple case is to use equation (62) for each estimate separately,

$$\begin{aligned} \hat{u}_k &\approx \frac{1}{1+\epsilon(\omega)}\frac{2}{n}\mathbf{C}_k^T\mathbf{y} \,, \\ \hat{v}_k &\approx \frac{1}{1-\epsilon(\omega)}\frac{2}{n}\mathbf{S}_k^T\mathbf{y} \,, \end{aligned} \tag{66}$$

where $\mathbf{C} = [\mathbf{C}_1, \mathbf{C}_2, \ldots, \mathbf{C}_m]$ and $\mathbf{S} = [\mathbf{S}_1, \mathbf{S}_2, \ldots, \mathbf{S}_m]$. The estimates in equation (66) correspond to setting all the off-diagonal terms in $\mathbf{C}^T\mathbf{C}$ and $\mathbf{S}^T\mathbf{S}$ equal to zero in equation (60).

The MLE of $\mathbf{u}$ and $\mathbf{v}$ can also be efficiently and simply estimated with the fast Fourier transform (FFT) of $\mathbf{y}$. The continuous Fourier transform (CFT) of $\mathbf{y}$, denoted by $Y(f)$, is

$$Y(f) = \sum_{i=1}^{n} e^{-2\pi j f t(i)} y_i \tag{67}$$

for $0 \leq f \leq 1/2$. Usually $t(i) = i - 1$ in equation (67), but for the comparison of different phase estimates, it is important to stay consistent. In practice, one can easily add a phase correction to equation (67) to account for any differences in the time indexes. The FFT—or more precisely, the discrete Fourier transform (DFT)—calculates equation (67) only at the center frequencies $F_k = k/n$ of the Fourier bins for $k = 0, 1, \ldots, (n-1)$. For each $\boldsymbol{\omega} = 2\pi\mathbf{f}$, one can obtain approximate estimates using the FFT, by rounding the frequencies to the nearest frequency bins:

$$\begin{aligned} \hat{u}_k &= \frac{2}{n}\mathrm{Re}\Big\{Y[\mathrm{round}(nf_k)/n]\Big\} \,, \\ \hat{v}_k &= -\frac{2}{n}\mathrm{Im}\Big\{Y[\mathrm{round}(nf_k)/n]\Big\} \,, \end{aligned} \tag{68}$$

where $\mathrm{round}(x)$ is the nearest integer to x. This procedure is equivalent to equation (57), with the harmonic frequencies rounded off to the nearest Fourier bin, which makes $\mathbf{X}^T\mathbf{X} = (n/2)\mathbf{I}$ (exactly). The MLE of the amplitude (of the harmonic at the nonrounded frequencies) can be obtained with equation (58), but to account for using the center frequency of the Fourier

bins rather than the exact frequencies, a better estimate of the phase (i.e., less biased) is

$$\hat{\phi}_k = \arctan(-\hat{v}_k, \hat{u}_k) - \Big[nf_k - \text{round}(nf_k)\Big]\pi\frac{n-1}{n}\,, \tag{69}$$

which can be a correction of almost $\pi/2$ for harmonic frequencies that are half a bin away from the center. Note that the approximate estimate equation (65) is equivalent to use of the CFT in equation (67) rather than the DFT, which leads to

$$\begin{aligned} \hat{u}_k &= \frac{2}{n}\text{Re}\Big[Y(f_k)\Big]\,, \\ \hat{v}_k &= -\frac{2}{n}\text{Im}\Big[Y(f_k)\Big]\,; \end{aligned} \tag{70}$$

this is simply equation (68) without rounding.

5. Gradient Descent Methods for Finding MLE

The MLE of the harmonic parameters can be found by gradient descent methods. Since for fixed frequencies, the MLE of the other parameters can be obtained with equation (60), these gradient descent methods are needed to find the MLE of the frequencies $\boldsymbol{\omega}$ or the fundamental frequency ω. Gradient descent methods can be implemented directly in terms of the amplitudes and phases, but this does not take advantage of the linearity of the parameterization in equation (5). The Newton-Raphson method uses an initial estimate $\hat{\boldsymbol{\theta}}_0$ and iteratively updates the estimate via

$$\hat{\boldsymbol{\theta}}_{k+1} = \hat{\boldsymbol{\theta}}_k - \left\{ \frac{\partial^2 \log[L(\mathbf{y}, \boldsymbol{\theta})]}{\partial \boldsymbol{\theta} \partial \boldsymbol{\theta}^T} \right\}^{-1} \left. \frac{\partial \log[L(\mathbf{y}, \boldsymbol{\theta})]}{\partial \boldsymbol{\theta}} \right|_{\boldsymbol{\theta} = \hat{\boldsymbol{\theta}}_k} , \tag{71}$$

which requires the inversion of the Hessian of the log-likelihood function. The gradient vector and the Hessian matrix in equation (71) can be written as

$$\frac{\partial \log[L(\mathbf{y}, \boldsymbol{\theta})]}{\partial \boldsymbol{\theta}} = \frac{1}{\sigma^2} \frac{\partial \mathbf{s}}{\partial \theta}^T \mathbf{e} , \tag{72}$$

and

$$\frac{\partial^2 \log[L(\mathbf{y}, \boldsymbol{\theta})]}{\partial \boldsymbol{\theta} \partial \boldsymbol{\theta}^T} = -\mathbf{I}(\boldsymbol{\theta}) + \mathbf{J}(\boldsymbol{\theta}) , \tag{73}$$

where the second component is

$$\mathbf{J}(\boldsymbol{\theta}) = \frac{1}{\sigma^2} \sum_{i=1}^{n} \frac{\partial^2 s_i}{\partial \boldsymbol{\theta}^2} e_i \tag{74}$$

and $\mathbf{I}$ is the information matrix defined by equation (12). An alternative to the Newton-Raphson method, called the *method of scoring*, is to replace the Hessian by its expected value; this method of scoring is often preferable because it involves less computation and has stabilizing properties. From equation (74), $E[\mathbf{J}(\boldsymbol{\theta})] = \mathbf{0}$, and the expected value of the Hessian is

$$E\left\{ \frac{\partial^2 \log[L(\mathbf{y}, \boldsymbol{\theta})]}{\partial \boldsymbol{\theta} \partial \boldsymbol{\theta}^T} \right\} = -I(\boldsymbol{\theta}) , \tag{75}$$

so that replacing the Hessian in equation (71) by equation (75) gives

$$\hat{\boldsymbol{\theta}}_{k+1} = \hat{\boldsymbol{\theta}}_k + I(\boldsymbol{\theta})^{-1} \left. \frac{\partial \log[L(\mathbf{y}, \boldsymbol{\theta})]}{\partial \boldsymbol{\theta}} \right|_{\boldsymbol{\theta} = \hat{\boldsymbol{\theta}}_k} , \tag{76}$$

which is the method of scoring. The method of scoring is presented by a derivation of the approximate diagonal information matrices for the parameterization with $\mathbf{u}$ and $\mathbf{v}$. These results are presented with different notation than that for amplitude and frequency, which has proven to be useful for implementation in MATLAB.

For the single harmonic case $\mathbf{s}(u, v, \omega) = \mathbf{C}u + \mathbf{S}v$, so that

$$\frac{\partial \mathbf{s}}{\partial \boldsymbol{\theta}} = \left[\begin{array}{cccc} \mathbf{C} & \mathbf{S} & \frac{\partial \mathbf{s}}{\partial \omega} \end{array} \right] , \tag{77}$$

where

$$\frac{\partial \mathbf{s}}{\partial \omega} = \frac{\partial \mathbf{C}}{\partial \omega} u + \frac{\partial \mathbf{s}}{\partial \omega} v \tag{78}$$

and

$$\begin{aligned} \left[\frac{\partial \mathbf{C}}{\partial \omega} \right]_i &= -t(i) \sin[\omega t(i)] , \\ \left[\frac{\partial \mathbf{S}}{\partial \omega} \right]_i &= t(i) \cos[\omega t(i)] \end{aligned} \tag{79}$$

are $n \times 1$ vectors of first derivatives obtained from equation (55). The information matrix is approximately diagonal

$$I(u, v, \omega) = \frac{1}{\sigma^2} \left[\begin{array}{ccc} \mathbf{C}^T\mathbf{C} & 0 & \mathbf{C}^T \frac{\partial \mathbf{s}}{\partial \omega} \\ 0 & \mathbf{S}^T\mathbf{S} & \mathbf{S}^T \frac{\partial \mathbf{s}}{\partial \omega} \\ \mathbf{C}^T \frac{\partial \mathbf{s}}{\partial \omega} & \mathbf{S}^T \frac{\partial \mathbf{s}}{\partial \omega} & \| \frac{\partial \mathbf{s}}{\partial \omega} \|^2 \end{array} \right] \approx \frac{n}{2\sigma^2} \left[\begin{array}{ccc} 1 & 0 & 0 \\ 0 & 1 & 0 \\ 0 & 0 & \frac{1}{12} A^2 n^2 \end{array} \right] , \tag{80}$$

which greatly simplifies the computation for each iteration in equation (76). For multiple harmonics with $\boldsymbol{\theta} = (\mathbf{u}, \mathbf{v}, \boldsymbol{\omega})$,

$$\frac{\partial \mathbf{s}}{\partial \boldsymbol{\theta}} = \left[\begin{array}{cccc} \mathbf{C} & \mathbf{S} & \frac{\partial \mathbf{s}}{\partial \omega_1} & \cdots \; \frac{\partial \mathbf{s}}{\partial \omega_m} \end{array} \right] , \tag{81}$$

where

$$\frac{\partial \mathbf{s}}{\partial \omega_k} = \frac{\partial \mathbf{C}_k}{\partial \boldsymbol{\omega}_k} u_k + \frac{\partial \mathbf{S}_k}{\partial \boldsymbol{\omega}_k} v_k \tag{82}$$

and generalizes equation (77). The information matrix is still approximately diagonal,

$$I(\mathbf{u}, \mathbf{v}, \boldsymbol{\omega}) \approx \frac{n}{2\sigma^2} \left[\begin{array}{ccc} \mathbf{I} & \mathbf{0} & \mathbf{0} \\ \mathbf{0} & \mathbf{I} & \mathbf{0} \\ \mathbf{0} & \mathbf{0} & n^2\mathbf{D}/12 \end{array} \right] , \tag{83}$$

where $\mathbf{D}$ is given in equation (27), which once again leads to efficient computation of each iteration in equation (76). The Hessian for the harmonic

case is similar to that of the multiple, except that it contains only one frequency parameter instead of m frequency parameters. With $\boldsymbol{\theta} = (\mathbf{u}, \mathbf{v}, \omega)$, $\frac{\partial \mathbf{s}}{\partial \boldsymbol{\theta}}$ can be written as in equation (77), but, in this case,

$$\frac{\partial \mathbf{s}}{\partial \omega} = \frac{\partial \mathbf{X}}{\partial \omega}\boldsymbol{\beta} = \frac{\partial \mathbf{C}}{\partial \omega}\mathbf{u} + \frac{\partial \mathbf{s}}{\partial \omega}\mathbf{v} \tag{84}$$

and

$$\begin{aligned} \left[\frac{\partial \mathbf{C}}{\partial \omega}\right]_{ij} &= -h_j t(i) \sin[h_j \omega t(i)] \,, \\ \left[\frac{\partial \mathbf{S}}{\partial \omega}\right]_{ij} &= h_j t(i) \cos[h_j \omega t(i)] \end{aligned} \tag{85}$$

are $n \times m$ matrices of first derivatives obtained from equation (55), with $\omega_k = h_k \omega$. The information matrix is once again approximately diagonal,

$$I(\mathbf{u}, \mathbf{v}, \omega) \approx \frac{n}{2\sigma^2} \begin{bmatrix} \mathbf{I} & \mathbf{0} & \mathbf{0} \\ \mathbf{0} & \mathbf{I} & \mathbf{0} \\ \mathbf{0} & \mathbf{0} & \frac{1}{12} n^2 \sum_{k=1}^{m} h_k^2 A_k^2 \end{bmatrix} , \tag{86}$$

and leads to an efficient implementation of equation (76) to estimate fundamental frequency.

As expected, the information matrices in equations (80), (83), and (86) lead to the same bounds for the frequency parameters in equations (17), (28), and (30), respectively. One can also get the approximate CRBs for $\mathbf{u}$ and $\mathbf{v}$,

$$\begin{aligned} CRB[\hat{u}_k] &\approx \frac{2\sigma^2}{n} \,, \\ CRB[\hat{v}_k] &\approx \frac{2\sigma^2}{n} \,, \end{aligned} \tag{87}$$

for both the multiple and harmonically related models. The CRBs in equation (87) are obtained exactly for the case when the frequency parameters are known.

Because of equation (57), methods can be developed for only the MLE of the frequency parameters. For the general multiple harmonic case, this is equivalent to finding ω to minimize

$$(\omega) = SS(\hat{\mathbf{u}}, \hat{\mathbf{v}}, \omega) = \mathbf{e}^T \mathbf{e} = \|\mathbf{y} - \mathbf{P}\mathbf{y}\|^2 = \|\mathbf{y}\|^2 - \mathbf{y}^T \mathbf{P} \mathbf{y} \,, \tag{88}$$

or, alternatively, to maximize the signal energy

$$E(\omega) = \mathbf{y}^T \mathbf{P} \mathbf{y} \,, \tag{89}$$

where

$$P = P_{\mathbf{X}} = \mathbf{X}(\mathbf{X}^T\mathbf{X})^{-1}\mathbf{X}^T \tag{90}$$

is the projection onto the subspace spanned by the columns of $\mathbf{X}(\omega)$. Note that $\mathbf{e}$, defined in equation (88), is the residual error at the optimal value.

Newton's method for estimating fundamental frequency is

$$\hat{\omega}_{k+1} = \hat{\omega}_k - \left(\frac{\partial SS^2}{\partial^2\omega}\right)^{-1} \frac{\partial SS}{\partial\omega}\bigg|_{\omega=\hat{\omega}_k}, \tag{91}$$

where $SS = SS(\omega)$ is given by equation (88) for the harmonically related case. To simplify the implementation of equation (91), I propose a decoupled procedure that first estimates the coefficients assuming fixed frequency, perhaps using an efficient approximation such as equation (68), and then optimizes frequency assuming fixed coefficients. It turns out that this procedure is equivalent to setting the cross-terms in the information matrix involving $(\mathbf{u}, \mathbf{v})$ and ω to zero in the method of scoring procedure for the coupled harmonic case. For example, the method of scoring for this approach simply becomes

$$\hat{\omega}_{k+1} = \hat{\omega}_k + \frac{\mathbf{e}^T\frac{\partial\mathbf{X}}{\partial\omega}\hat{\boldsymbol{\beta}}}{\|\frac{\partial\mathbf{X}}{\partial\omega}\hat{\boldsymbol{\beta}}\|^2}, \tag{92}$$

where, as mentioned before, $\hat{\boldsymbol{\beta}}$ can be an approximate MLE of the coefficients to conserve computation. It is important to note that defining the phase in the middle of the time window is not just a matter of convenience in this case, but is absolutely necessary for the performance of this decoupled estimation procedure.

6. Colored Noise

Now I consider the case where Z is no longer assumed white, but instead wide-sense stationary (WSS) Gaussian with a known covariance of $K_{ZZ}(k)$ and

$$\sigma^2(\omega) = P_{ZZ}(\omega) = \sum_{k=-\infty}^{\infty} e^{-j\omega k} K_{ZZ}(k) \tag{93}$$

is the power spectral density or *local noise variance*. If the noise vector $\mathbf{z}$ in equation (8) is multivariate Gaussian $N_n(\mathbf{0}, \mathbf{\Sigma})$, where $\mathbf{\Sigma}_{ij} = K_{ZZ}(i-j)$, then

$$\mathbf{I}(\boldsymbol{\theta}) = \frac{\partial \mathbf{s}}{\partial \boldsymbol{\theta}}^T \mathbf{\Sigma}^{-1} \frac{\partial \mathbf{s}}{\partial \boldsymbol{\theta}} \tag{94}$$

is the information matrix. Approximate results in the colored Gaussian noise case can be obtained with the following approximation, which is valid for large enough n and under mild assumptions on $\sigma^2(\omega)$

$$\mathbf{a}^T \mathbf{\Sigma}^{-1} \mathbf{b} \approx \frac{1}{2\pi} \int_{-\pi}^{\pi} \frac{A(\omega) B^*(\omega)}{\sigma^2(\omega)} \, d\omega \, , \tag{95}$$

where $\mathbf{a}$ and $\mathbf{b}$ are $n \times 1$ vectors with continuous Fourier transforms (i.e., equation (67)) $A(\omega)$ and $B(\omega)$, respectively. With the use of equation (95) for the case of estimating multiple and coupled harmonics, the vectors often asymptotically have discrete spectra, and the approximation can be evaluated quickly by the notion of delta functions or more rigorously by the measure-theoretic interpretation of the integral. An important point to realize about this approximation is that, depending on the nature of the covariance function, it may require a larger n to become valid than is given in equation (47).

An interesting result of equation (95) (or methods used by Ghogho and Swami [8]), is that, under mild assumptions, the CRBs for the colored Gaussian noise case are approximately equal to those in equations (28) and (30), with $\sigma^2 = \sigma^2(h_k \omega)$ and

$$\rho_k = \frac{A_k^2}{2\sigma^2(h_k \omega)} \tag{96}$$

the *local SNR*. The dependence on local SNR can be seen heuristically by noting that the spectral density for the partial derivative of $\mathbf{s}$ with any of the harmonic signal model parameters will asymptotically have all its mass

concentrated at the corresponding frequency, and, by equation (95), the entry in the information matrix will depend only on the local noise variance. The MLE for colored Gaussian noise is

$$\hat{\boldsymbol{\beta}} = (\mathbf{X}^T\boldsymbol{\Sigma}^{-1}\mathbf{X})^{-1}\mathbf{X}^T\boldsymbol{\Sigma}^{-1}\mathbf{y}\,, \tag{97}$$

which generalizes equation (57). Using equation (95), it can be shown that

$$\begin{aligned}\mathbf{C}^T\boldsymbol{\Sigma}^{-1}\mathbf{S} &\approx \mathbf{0}\\ \mathbf{S}^T\boldsymbol{\Sigma}^{-1}\mathbf{C} &\approx \mathbf{0}\,,\end{aligned} \tag{98}$$

and equation (97) separates into the cosine and sine components and in the same way as equation (60). Further,

$$\mathbf{C}^T\boldsymbol{\Sigma}^{-1}\mathbf{C} \approx \mathbf{S}^T\boldsymbol{\Sigma}^{-1}\mathbf{S} \approx \frac{n}{2}\mathrm{diag}\Big[1/\sigma^2(\omega_1),\ 1/\sigma^2(\omega_1),\ \ldots,\ 1/\sigma^2(\omega_m)\Big] \tag{99}$$

and

$$\begin{aligned}\mathbf{C}_k^T\boldsymbol{\Sigma}^{-1}\mathbf{y} &\approx \mathbf{C}_k^T\mathbf{y}/\sigma^2(\omega_k)\,,\\ \mathbf{S}_k^T\boldsymbol{\Sigma}^{-1}\mathbf{y} &\approx \mathbf{S}_k^T\mathbf{y}/\sigma^2(\omega_k)\,,\end{aligned} \tag{100}$$

so that

$$\begin{aligned}u_k &\approx \Big[2\sigma^2(\omega_k)/n\Big]\Big[\mathbf{C}_k^T\mathbf{y}/\sigma^2(\omega_k)\Big] = (2/n)\mathbf{C}_k^T\mathbf{y}\,,\\ v_k &\approx \Big[2\sigma^2(\omega_k)/n\Big]\Big[\mathbf{S}_k^T\mathbf{y}/\sigma^2(\omega_k)\Big] = (2/n)\mathbf{S}_k^T\mathbf{y}\,,\end{aligned} \tag{101}$$

which is exactly the same approximation as equation (65) and the CFT estimates, equation (70). In a similar manner, the DFT estimates in equation (68) and the estimates in equation (66) are approximately valid in the colored noise. So asymptotically, estimating multiple harmonic in colored noise completely decouples into estimating m single harmonics in white noise with variance equal to the local noise variance at that harmonic.

7. Coupled Harmonic Model for Battlefield Acoustic Targets

Target identification using battlefield acoustic sensor arrays is an important problem for the Army [9]. Acoustic signatures of targets of interest, such as tanks and trucks, exhibit time-varying patterns of harmonic amplitudes that facilitate target ID. The spectrogram from one of an array of seven acoustic sensors taken by the Army Research Laboratory (ARL) during recent field tests at Aberdeen Proving Ground (APG), Maryland, is shown in figure 1. The sampling rate is T = 2000 samples/s and FFTs were taken with n = 2048 samples. The target is an M60 tank that is approaching the sensor until the time of the closest point of approach (CPA), at approximately t = 40 s, and retreating afterwards. The range at CPA is approximately 50 m.

The harmonic structure and the time-varying nature of the signal are very apparent. The strongest line at approximately 90 Hz is the sixth harmonic, so that the fundamental frequency is approximately 15 Hz. A coupled harmonic signal model accurately models a large portion of a vehicle's acoustic signature, especially that coming from the engine. For the current ARL target ID system [10], the second through twelfth harmonics are used so that

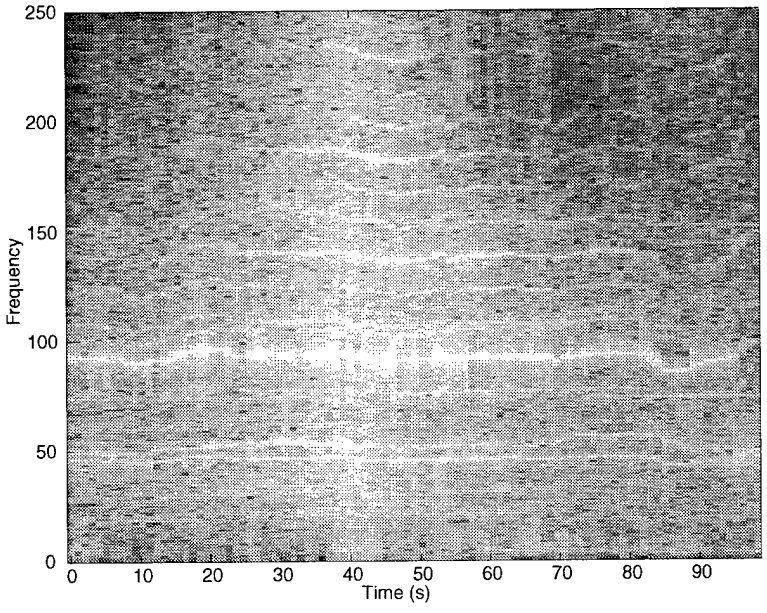

Figure 1. Battlefield acoustic data with time-varying coupled harmonic signal.

$\mathbf{h} = (2, 3, 4, 5, 6, 7, 8, 9, 10, 11, 12)^T$ and $m = 11$ in equation (6). The additive noise process Z in equation (7) consists of the cumulative effect of ambient noise such as wind, broadband and narrowband nontarget sources, and a portion of the target's acoustic signature not completely described by equation (6), such as the additional line at approximately 50 Hz in figure 1, which is coming from the track slap. An example of data from a short time window (approximately 0.25 s) is shown in figure 2, which shows the first 512 samples from the same data as in figure 1. For battlefield acoustic scenarios, the fundamental frequency can be assumed constant for short time windows (on the order of 1 s), and the stationary methods presented can be applied.

7.1 Fundamental Frequency Estimators and Trackers

For each fundamental frequency f, the residual error of the coupled harmonic signal model can be efficiently and simply estimated by the FFT of $\mathbf{y}$, with $f_k = h_k\omega/(2\pi)$ in equation (68). In practice, the search for the fundamental frequency is limited over a small range of values, e.g., 5 to 20 Hz in increments of 0.1 Hz. A plot of the residual error power SS/n in equation (88) for the data in figure 2 (the true fundamental frequency is approximately f = 15.5 Hz) is shown in figure 3. A series of clear regions of minimum power shows, in this case, that the fundamental frequency needs to be known initially to within a certain accuracy (roughly 5 Hz) to guarantee that this method finds the correct local minimum. Once a fundamental

Figure 2. Acoustic data with coupled harmonic signal.

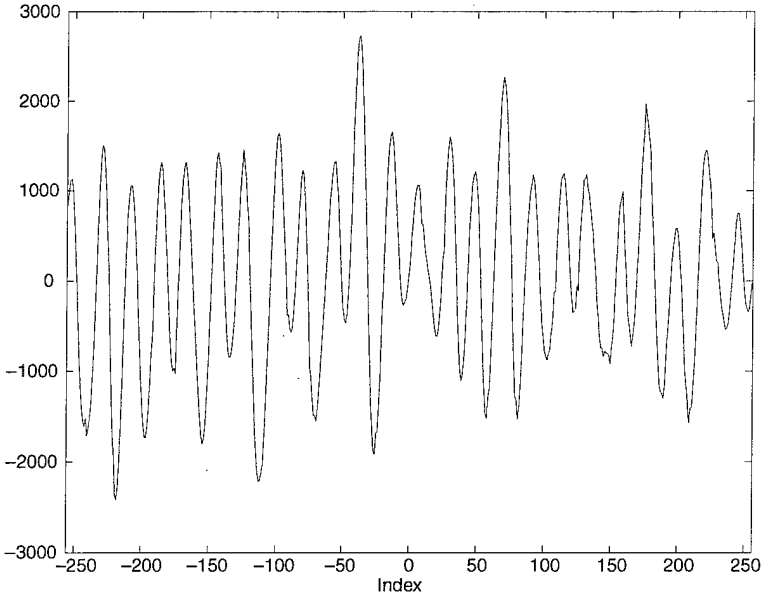

frequency is estimated, the estimate of amplitude can be readily found, although it is important to use the corrected estimate of the phase in equation (69). The fundamental frequency can be estimated more accurately with the exact MLE. A plot of the residual error power for the MLE of the data in figure 2 (assuming white Gaussian noise) is shown in figure 4. The plot is similar to figure 3, except that the maximum values are much sharper, which suggests that the MLE estimate will be much more accurate.

Figure 3. Residual error power for FFT fundamental frequency estimation.

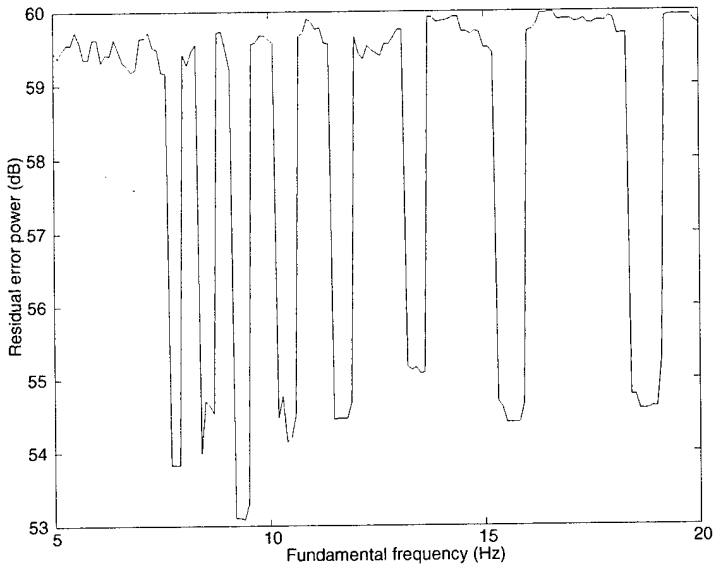

Figure 4. Residual error power for MLE fundamental frequency estimation.

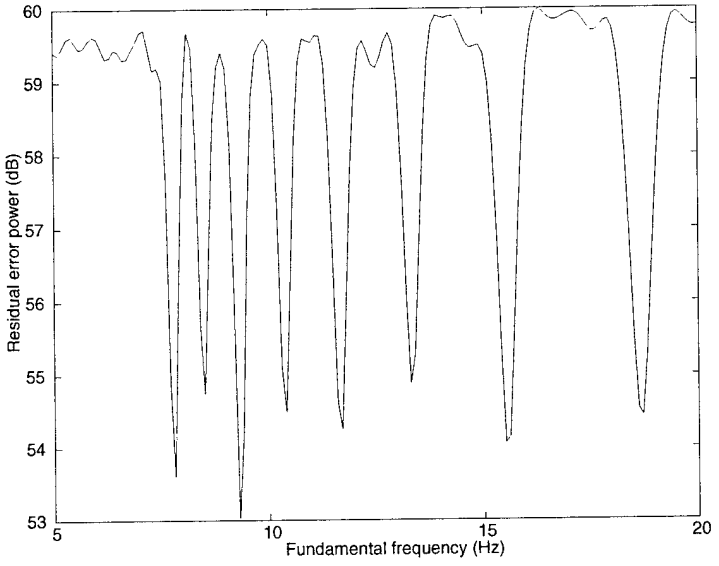

Figures 3 and 4 suggest that a simple but effective fundamental frequency tracker can be constructed, assuming an accurate initial value has been obtained. Subsequent estimates can be obtained if one minimizes equation (3) over a range of fundamental frequencies equal to the previous estimate plus a reduced number of offsets reflecting the maximum expected change over the time window. For the data in equation (1), accurate estimates of the fundamental frequency were efficiently obtained using FFTs with this approach, an initial value of 15.5 Hz, offsets of -0.25 to 0.25 Hz in increments of 0.025 Hz, and time windows of length n = 2048 with 75 percent overlap. The iterative procedures using the gradient descent methods described previously can be modified slightly to track fundamental frequencies by an adaptive filter. For the data in equation (1), this approach tracked the fundamental frequency accurately for most of the run, but did lose the signal for the last 10 s or so, where the signature changed significantly.

7.2 Harmonic Amplitudes and Phases for Target Identification

Using the estimates of fundamental frequency obtained from the tracker described above, I obtained estimates of amplitude and phase for the data in figure 1 using equation (60). Figure 5 shows the estimated amplitudes of the third and sixth harmonics; despite the variation in power as a function of range due to acoustic propagation effects, these amplitudes have a fairly constant difference. This suggests that the ratio of the third and sixth harmonics (the strongest line) is a more robust feature for target ID. For this reason, normalizing the amplitudes by the strongest line is part of ARL's current target ID system.

A phase coupling also exists between the third and sixth harmonics, as shown in figure 6, which is a plot of the difference

$$d_{36} = \text{mod}(2\phi_3 - \phi_6,\ 2\pi) \tag{102}$$

versus time. The value of d_{36} is relatively constant over short time windows. However, the difference is not zero, as predicted in some models (e.g., see Swami and Ghogho [7]), and it does appear to vary slightly over the entire time period. This apparent anomaly is perhaps due to propagation effects and/or variations in the target's aspect or operation characteristics. The extent to which differences such as in equation (102) are useful in target identification remains an open issue, as does the accuracy with which these differences can be estimated. One reason the harmonic numbers 3 and 6 were chosen to show coupling is that the simple 2 to 1 ratio between them minimizes the variance of the corresponding difference. With harmonics 5 and 7, for example, the corresponding difference is $d_{57} = \text{mod}(7\phi_5 - 5\phi_7, 2\pi)$ which, with all else being equal, would have a

Figure 5. Harmonic amplitude estimates.

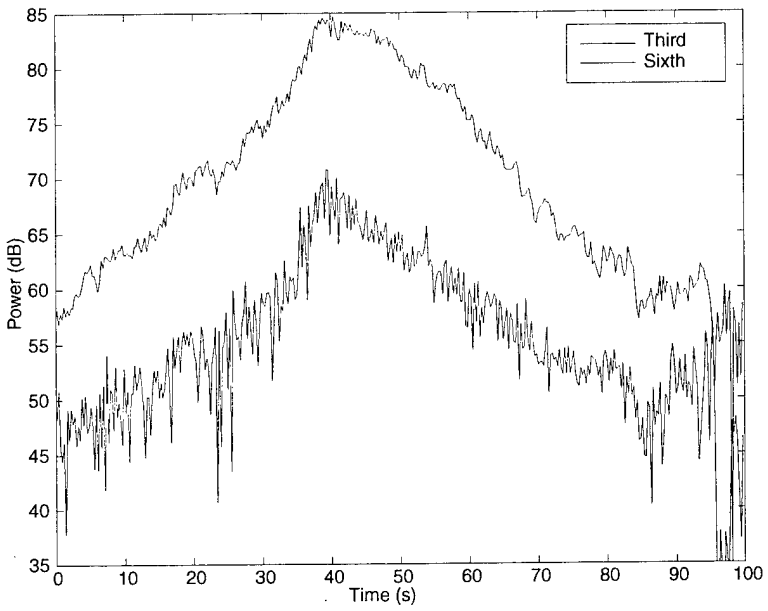

Figure 6. Phase coupling between third and sixth harmonics.

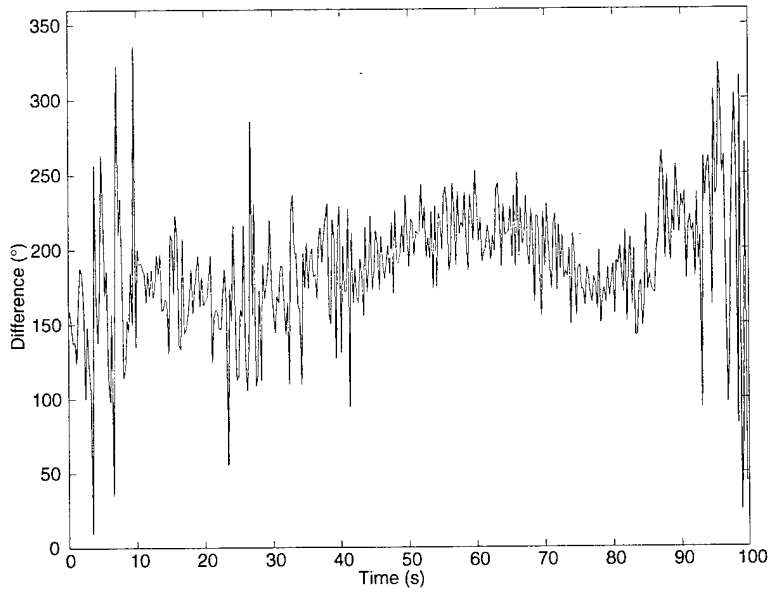

variance 18.5 times that of equation (102). So, for targets where 5 and 7 are dominant harmonic lines, the harmonic coupling will be more difficult to detect and track and may not be a stable feature.

The importance of using the corrected phase in equation (69) can be demonstrated in the calculation of equation (102). Without the correction, empirical results showed that half the time the calculated differences were about

180° off (i.e., the worst possible error), and were nearly correct the other half. The reason for this, assuming uniform distribution within the Fourier frequency bins, is that half the time the errors in the phase estimates are in opposite directions and add together destructively in equation (102), and half the time they cancel each other out.

For large n, the variance of the MLEs of amplitude, phase, and fundamental frequency are approximately equal to the CRB. Looking at equation (30), the variance of fundamental frequency goes down with the presence of high SNR tones with large harmonic numbers. For battlefield acoustics, this is not always the case, because increased propagation loss occurs at higher frequencies. Also, the fundamental frequency can be estimated fairly accurately with small data sizes, but equation (21) shows that exploiting the harmonic phase coupling for target ID may require more time samples. However, because of the nonstationarity of the fundamental frequency, it is not always possible to increase n arbitrarily, and the accuracy of phase estimates is limited with stationary approaches. So, obtaining more accurate phase estimates with time-varying fundamental frequency is a subject for further research and presents an interesting problem in nonstationary signal processing.

8. Conclusions

Efficient methods for the maximum likelihood estimation of parameters for multiple and coupled harmonics were presented that exploit the diagonality of the information matrices when the phase is defined in the middle of the time window. With the generalization to local noise variances and local SNRs, the CRBs for the colored noise case are asymptotically equivalent to the white noise case, perhaps requiring a larger number of samples n. With the same caveat, the approximate MLE methods for the white noise case are also applicable to the colored noise case. The MLE methods were applied to real battlefield acoustic data and the problem of target identification. The difference between the power levels of strong harmonics was shown to be fairly constant over the entire run, which demonstrates the potential robustness of these features. Harmonic phase coupling was also shown to be present in these acoustic signatures, although challenges remain to fully exploit these relationships for target ID. For example, with all else being equal, frequencies with simple harmonic relationships, such as 2 to 1 or 3 to 2, are preferred to produce stable features. Also, naive use of FFT approaches to estimate phase leads to erratic estimates. The CRBs presented provide insights into the limitations of the accuracy of phase-coupling estimates and suggests the value of developing nonstationary methods.

References

1. D. C. Rife and R. R. Boorstyn, "Single-tone parameter estimation from discrete-time observations," *IEEE Trans. Inform. Theory* **IT-20**, pp. 591–598, September 1974.

2. D. C. Rife and R. R. Boorstyn, "Multiple tone parameter estimation from discrete-time observations," *Bell Syst. Tech J.*, pp. 1389–1410, November 1976.

3. P. Stoica, R. L. Moses, B. Friedlander, and T. Soderstrom, "Maximum likelihood estimation of the parameters of multiple sinusoids from noisy measurements," *IEEE Trans. Acoust. Speech Signal Process.* **37**, pp. 378–392, March 1989.

4. B. Porat, *Digital Processing of Random Signals: Theory & Methods*, Prentice Hall, 1994.

5. G. Zhou and G. Giannakis, "Harmonics in Gaussian multiplicative and additive noise: Cramer-Rao bounds," *IEEE Trans. Signal Process.* **43**, pp. 1217–1231, May 1995.

6. S. M. Kay, *Fundamentals of Statistical Signal Processing: Estimation Theory*, PTR Prentice Hall, Englewood Cliffs, New Jersey, 1993.

7. A. Swami and M. Ghogho, "Cramer-Rao bounds for coupled harmonics in noise," *Proc. Asilomar Conf. Sig. Sys. Comp.*, 1997.

8. M. Ghogho and A. Swami, "Lower bounds on the estimation of harmonics in colored noise," *Proc. Asilomar Conf. Sig. Sys. Comp.*, 1997.

9. N. Srour and J. Robertson, *Remote Netted Acoustic Detection System*, Army Research Laboratory, ARL-TR-706, May 1995.

10. M. Wellman, N. Srour, and D. Hills, *Acoustic Feature Extraction for a Neural Network Classifier*, Army Research Laboratory, ARL-TR-1166, January 1997.

Distribution

Admnstr
Defns Techl Info Ctr
Attn DTIC-OCP
8725 John J Kingman Rd Ste 0944
FT Belvoir VA 22060-6218

Ofc of the Secy of Defns
Attn ODDRE (R&AT)
The Pentagon
Washington DC 20301-3080

Ofc of the Secy of Defns
Attn OUSD(A&T)/ODDR&E(R) R J Trew
Washington DC 20301-7100

AATD (ATCOM)
Attn AMSAT-R-TU L Sutton
FT Eustis VA 22604

AMCOM MRDEC
Attn AMSMI-RD W C McCorkle
Redstone Arsenal AL 35898-5240

Army Spc and Strtgc Defns
Attn CSSD-TC-C R N Adams
PO Box 1500
Huntsville AL 35807-3801

CECOM
Attn PM GPS COL S Young
FT Monmouth NJ 07703

Dir for MANPRINT
Ofc of the Deputy Chief of Staff for Prsnnl
Attn J Hiller
The Pentagon Rm 2C733
Washington DC 20301-0300

INSCOM
Dept of the Army
Attn L Schmidt
Attn B Kitchen
Attn E Bielecki
8825 Beulah Stret
FT Belvoir VA 22060-5246

US Army AFDD
Attn AMSAT-R-AF D Boxwell
Ames Rsrch MS N215-1
Moffett Field CA 94035

US Army ARDEC
Attn AMSTA-AR-FSF-RM J Heberley
Bldg 95N
Picatinny Arsenal NJ 07806

US Army Materiel Command
Principal Deputy for Technology
Attn W Kitchens
5001 Eisenhower Avenue
Alexandria VA 22333-0001

US Army Materiel Command
Assistant Deputy Chief of Staff for Research
and Development
Attn AMCRDA-T R Price
5001 Eisenhower Avenue
Alexandria VA 22333-0001

Department of the Army
Assistant Secretary of the Army
Attn SAAL-TR R Morrison
Attn SAAL-ZT M Andrews
Attn SAAL-TT L Stotts
2511 Jefferson Davis Highway Ste 980
Arlington VA 22333-0001

US Army ARDEC
Attn AMSTA-AR-TD M Fisette
Bldg 1
Picatinny Arsenal NJ 07806-5000

US Army CERDEC, NVESD
Attn AMSEL-RD-NV-VISP-CR G Klager
FT Belvoir VA 22060

US Army CRREL
Attn CECL-GP M Moran
72 Lyme Rd
Hanover NH 03755-1290

US Army Edgewood RDEC
Attn SCBRD-TD G Resnick
Aberdeen Proving Ground MD 21010-5423

US Army Info Sys Engrg Cmnd
Attn ASQB-OTD F Jenia
FT Huachuca AZ 85613-5300

Distribution (cont'd)

US Army Natick RDEC Acting Techl Dir
Attn SSCNC-T P Brandler
Natick MA 01760-5002

US Army NVESD
Attn AMSEL-RD-NV-TIS-PS D Rehak
Attn AMSRL-RD-NV-SS-GV R Volpone
10221 Burbeck Rd Ste 430
FT Belvoir VA 22060-5806

US Army Simulation, Train, & Instrmntn Cmnd
Attn J Stahl
12350 Research Parkway
Orlando FL 32826-3726

US Army TACOM
Attn AMSTA-TR-S E Shalis
Warren MI 48090

US Army TACOM
Attn AMSTA-JCS D Thomas
Attn AMSTA-TA J Chapin
Warren MI 48397-5000

US Army Train & Doctrine Cmnd
Battle Lab Integration & Techl Dirctrt
Attn ATCD-B J A Klevecz
FT Monroe VA 23651-5850

US Military Academy
Mathematical Sci Ctr of Excellence
Attn MDN-A LTC M D Phillips
Dept of Mathematical Sci Thayer Hall
West Point NY 10996-1786

USA NGIC
Attn SRA-ELLIOTT C Elliott
220 7th Stret NE
Charlottesville VA 22902

Waterways Experiment Station
Attn L Kestler
3909 Halls Ferry Road
Vicksburg MS 39180

Nav Surface Warfare Ctr
Attn G33 T Holland
Attn Code B07 J Pennella Bldg 1470 Rm 1101
Attn Code F41 T Saffos
Attn Code T41/Dahlgren Div R G Gross
17320 Dahlgren Rd
Dahlgren VA 22448-5100

Naval Undersea Warfare Ctr
Attn Code 2121 R Rowland
New London CT 06320

Ofc of Naval Rsrch
Attn Code 342 H Hawkins
Attn Code 321 J Tague
Attn Code 311 W Martinez
800 N Quincy Street
Arlington VA 22217-5660

Chicken Little Joint Proj
Attn 46 OG/OGML J A Sledge
104 Cherokee Ave
Eglin AFB FL 32542-5600

DARPA
Attn E Carapezza
Attn S Welby
3701 N Fairfax Dr
Arlington VA 22203-1714

Boston University
Dept of Biomedical Engrg
Attn D Mountain
44 Cummington Street
Boston MA 02215

Georgia Tech Rsrch Inst
Rsrch Security Dept
Attn J Echard
Atlanta GA 30332

Johns Hopkins Univ
Applied Physics Lab
Attn A Coon
Attn J Sari
Johns Hopkins Rd
Laurel MD 20723-6099

Distribution (cont'd)

Morgan State Univ
Dept EE
Attn J Whitney
Mitchell Eng Bldg
5200 Perring Parkway
Baltimore MD 21239

Univ of CA at Los Angeles
Elect Engrg Dept
Attn K Yao
Attn B Kaiser
Engineering IV Bldg
Los Angeles CA 90095-1594

Univ of Maryland
Elect Engr Dept
Attn J S Baras
RM 2249 AV Williams Bldg
College Park MD 20742-3275

Univ of Maryland
Elect Engrg Dept
Attn S Shamma
College Park MD 20742-3275

Univ of Mississippi
NCPA
Attn H E Bass
University MS 38577

Univ of Mississippi
Dept of Physics and Astronomy
Attn R Raspet
University MS 38577

Univ of Texas
Appld Rsrch Lab
Attn M B Bennett
PO Box 8029
Austin TX 78713-8029

Univ of Washington
Attn Dept EE/FT-10 L Atlas
PO Box 352500
Seattle WA 98195-2500

Univ of Maryland
Inst of Systems Rsrch
Attn D Depireux
College Park MD 20742-3275

Univ of Virginia
Department of Statistics
Attn D Lake (25 copies)
111 Halsey Hall
Charlottesville VA 22903

George Mason Univ
Dept of Appl and Eng Statistics
Attn MS 4A7 K L Bell
Fairfax VA 22030-4444

Draper Labs
Attn MS 37 P Rosenstrach
Attn MS 53 K Houston
555 Technology Sq
Cambridge MA 02139

Harry L. Hurd Assoc Inc
Attn H L Hurd
309 Moss Run
Raleigh NC 27614

Hicks & Associates Inc
Attn G Singley III
1710 Goodrich Dr Ste 1300
McLean VA 22102

IIT Rsrch Inst
Attn J Robertson
4600 Forbes Blvd 2nd floor
Lanham MD 20706

Lockheed Sanders Inc
Attn S W Lang
PO Box 2057
Nashua NH 03061-0868

Lockheed Sanders Inc
Attn PTP02-A001 D Deadrick
PO Box 868
Nashua NH 03061-0868

MCQ Assoc Inc
Attn R Thomas
PO Box 8322 1551 Forbes Street
Fredericksburg VA 22405

MIT Lincoln Lab
Attn S4-307B R Lacoss
244 Wood Stret
Lexington MA 02173-9108

Distribution (cont'd)

Northrop Corp
Attn R Duff
PO Box 5032
Hawthrone CA 90251-5032

Palisades Inst for Rsrch Svc Inc
Attn E Carr
1745 Jefferson Davis Hwy Ste 500
Arlington VA 22202-3402

Rockwell Intrntl Corp Control & Infor Mgmt
Attn L P Clare
Attn H O Marcy
1049 Camino Dos Rios
Thousand Oaks CA 91360

Textron Sys Div
Subsidiary of Textron Inc
Attn R L Steadman
201 Lowell Stret
Wilmington MA 01887

Army Rsrch Lab/SLAD
Attn AMSRL-SL-EV J Williams
Bldg 1630
White Sands Missile Range NM 88002-5513

US Army Rsrch Lab/HRED
Attn AMSRL-HR-SD J Kalb Bldg 520 Rm 28
Aberdeen Proving MD 21005

Army Rsrch Ofc
Atmos Sci Branch
Attn AMSRL-RO-EN W D Bach Jr
PO Box 12211
Research Triangle Park NC 27709-2211

Army Rsrch Ofc
Physics Div
Attn AMSRL-RO-EM Assoc Dir
Math & Computer Sci Div R Launer
PO Box 12211
Research Triangle Park NC 27709-2211

Director
US Army Rsrch Ofc
4300 S Miami Blvd
Research Triangle Park NC 27709

US Army Rsrch Ofc
Attn AMSRL-RO-PP M Ciftan
PO Box 12211
Research Triangle Park NC 27709-2211

US Army Rsrch Ofc
Attn AMSRL-RO-EM J Lavery
4300 South Miami Blvd
Durham NC 27703

US Army Rsrch Lab
Attn AMSRL-DD J Rocchio
Attn AMSRL-CI-AS Mail & Records Mgmt
Attn AMSRL-CI-AT Techl Pub (3 copies)
Attn AMSRL-CI-LL Techl Lib (3 copies)
Attn AMSRL-IS-EE D K Wilson
Attn AMSRL-IS-EE H J Auvermann
Attn AMSRL-BE-S J M Noble
Attn AMSRL-SE-SA N Srour (5 copies)
Adelphi MD 20783-1197

REPORT DOCUMENTATION PAGE

Form Approved
OMB No. 0704-0188

1. AGENCY USE ONLY *(Leave blank)*	2. REPORT DATE	3. REPORT TYPE AND DATES COVERED
	December 1999	Final, Sept. 1997 to Mar. 1998

4. TITLE AND SUBTITLE Efficient Maximum Likelihood Estimation for Multiple and Coupled Harmonics

5. FUNDING NUMBERS
DA PR: AH16
PE: 62120A

6. AUTHOR(S) Douglas Lake

ARL POC: Nino Srour, 394-2623

7. PERFORMING ORGANIZATION NAME(S) AND ADDRESS(ES)
U.S. Army Research Laboratory
Attn: AMSRL-SE-SA email: nsrour@arl.mil
2800 Powder Mill Road
Adelphi, MD 20783-1197

8. PERFORMING ORGANIZATION REPORT NUMBER
ARL-TR-2014

9. SPONSORING/MONITORING AGENCY NAME(S) AND ADDRESS(ES)
U.S. Army Research Laboratory
2800 Powder Mill Road
Adelphi, MD 20783-1197

10. SPONSORING/MONITORING AGENCY REPORT NUMBER

11. SUPPLEMENTARY NOTES
ARL PR: 8NE4TT
AMS code: 622120.H16
Douglas Lake is an American Society of Engineering Education postdoctoral fellow at ARL.

12a. DISTRIBUTION/AVAILABILITY STATEMENT
Approved for public release; distribution unlimited.

12b. DISTRIBUTION CODE

13. ABSTRACT *(Maximum 200 words)*

The maximum likelihood estimates (MLEs) and Cramer-Rao bounds (CRBs) for parameters of harmonics in Gaussian noise have been well studied. If the phase of the signal is defined in the middle of the time interval rather than at the beginning (as is more common), the information matrix is approximately diagonal, and the formulation and analysis of the MLEs and CRBs are simplified. More significantly, this simple modification decouples the estimation of phase and frequency and leads to efficient MLE gradient descent algorithms. In this report, these MLE procedures and CRB analysis are presented for the multiple and coupled harmonic case, as well as for colored noise. A new criterion on the required sample size is presented to give uniform bounds on the accuracy of diagonal information matrix approximation; uniform bounds are needed to ensure the effectiveness of the gradient descent methods. These methods are demonstrated on real data from battlefield acoustic sensors, where they can be used to help identify targets of interest, such as tanks or trucks.

14. SUBJECT TERMS	15. NUMBER OF PAGES
Fundamental frequency, coupled harmonics	42
	16. PRICE CODE

17. SECURITY CLASSIFICATION OF REPORT	18. SECURITY CLASSIFICATION OF THIS PAGE	19. SECURITY CLASSIFICATION OF ABSTRACT	20. LIMITATION OF ABSTRACT
Unclassified	Unclassified	Unclassified	UL

NSN 7540-01-280-5500

Standard Form 298 (Rev. 2-89)
Prescribed by ANSI Std. Z39-18
298-102